Absence of Suppression in Particle Production at Large Transverse Momentum in $\sqrt{s_{NN}} = 200$ GeV d + Au Collisions

S. S. Adler,[4] S. Afanasiev,[19] C. Aidala,[9] N. N. Ajitanand,[43] Y. Akiba,[20,39] A. Al-Jamel,[34] J. Alexander,[43] K. Aoki,[24]
L. Aphecetche,[45] R. Armendariz,[34] S. H. Aronson,[4] R. Averbeck,[44] T. C. Awes,[35] V. Babintsev,[16] A. Baldisseri,[10]
K. N. Barish,[5] P. D. Barnes,[27] B. Bassalleck,[33] S. Bathe,[5,30] S. Batsouli,[9] V. Baublis,[38] F. Bauer,[5] A. Bazilevsky,[4,40]
S. Belikov,[18,16] M. T. Bjorndal,[9] J. G. Boissevain,[27] H. Borel,[10] M. L. Brooks,[27] D. S. Brown,[34] N. Bruner,[33] D. Bucher,[30]
H. Buesching,[4,30] V. Bumazhnov,[16] G. Bunce,[4,40] J. M. Burward-Hoy,[27,26] S. Butsyk,[44] X. Camard,[45] P. Chand,[3]
W. C. Chang,[2] S. Chernichenko,[16] C. Y. Chi,[9] J. Chiba,[20] M. Chiu,[9] I. J. Choi,[52] R. K. Choudhury,[3] T. Chujo,[4]
V. Cianciolo,[35] Y. Cobigo,[10] B. A. Cole,[9] M. P. Comets,[36] P. Constantin,[18] M. Csanád,[12] T. Csörgő,[21] J. P. Cussonneau,[45]
D. d'Enterria,[9] K. Das,[13] G. David,[4] F. Deák,[12] H. Delagrange,[45] A. Denisov,[16] A. Deshpande,[40] E. J. Desmond,[4]
A. Devismes,[44] O. Dietzsch,[41] J. L. Drachenberg,[1] O. Drapier,[25] A. Drees,[44] A. Durum,[16] D. Dutta,[3] V. Dzhordzhadze,[46]
Y. V. Efremenko,[35] H. En'yo,[39,40] B. Espagnon,[36] S. Esumi,[48] D. E. Fields,[33,40] C. Finck,[45] F. Fleuret,[25] S. L. Fokin,[23]
B. D. Fox,[40] Z. Fraenkel,[51] J. E. Frantz,[9] A. Franz,[4] A. D. Frawley,[13] Y. Fukao,[24,39,40] S.-Y. Fung,[5] S. Gadrat,[28]
M. Germain,[45] A. Glenn,[46] M. Gonin,[25] J. Gosset,[10] Y. Goto,[39,40] R. Granier de Cassagnac,[25] N. Grau,[18] S. V. Greene,[49]
M. Grosse Perdekamp,[17,40] H.-Å. Gustafsson,[29] T. Hachiya,[15] J. S. Haggerty,[4] H. Hamagaki,[7] A. G. Hansen,[27]
E. P. Hartouni,[26] M. Harvey,[4] K. Hasuko,[39] R. Hayano,[7] X. He,[14] M. Heffner,[26] T. K. Hemmick,[44] J. M. Heuser,[39]
P. Hidas,[21] H. Hiejima,[17] J. C. Hill,[18] R. Hobbs,[33] W. Holzmann,[43] K. Homma,[15] B. Hong,[22] A. Hoover,[34]
T. Horaguchi,[39,40,47] T. Ichihara,[39,40] V. V. Ikonnikov,[23] K. Imai,[24,39] M. Inuzuka,[7] D. Isenhower,[1] L. Isenhower,[1]
M. Issah,[43] A. Isupov,[19] B. V. Jacak,[44] J. Jia,[44] O. Jinnouchi,[39,40] B. M. Johnson,[4] S. C. Johnson,[26] K. S. Joo,[31] D. Jouan,[36]
F. Kajihara,[7] S. Kametani,[7,50] N. Kamihara,[39,47] M. Kaneta,[40] J. H. Kang,[52] K. Katou,[50] T. Kawabata,[7] A. Kazantsev,[23]
S. Kelly,[8,9] B. Khachaturov,[51] A. Khanzadeev,[38] J. Kikuchi,[50] D. J. Kim,[52] E. Kim,[42] G.-B. Kim,[25] H. J. Kim,[52]
E. Kinney,[8] A. Kiss,[12] E. Kistenev,[4] A. Kiyomichi,[39] C. Klein-Boesing,[30] H. Kobayashi,[40] V. Kochetkov,[16] R. Kohara,[15]
B. Komkov,[38] M. Konno,[48] D. Kotchetkov,[5] A. Kozlov,[51] P. J. Kroon,[4] C. H. Kuberg,[1] G. J. Kunde,[27] K. Kurita,[39]
M. J. Kweon,[22] Y. Kwon,[52] G. S. Kyle,[34] R. Lacey,[43] J. G. Lajoie,[18] Y. Le Bornec,[36] A. Lebedev,[18,23] S. Leckey,[44]
D. M. Lee,[27] M. J. Leitch,[27] M. A. L. Leite,[41] X. Li,[6] X. H. Li,[5] H. Lim,[42] A. Litvinenko,[19] M. X. Liu,[27] C. F. Maguire,[49]
Y. I. Makdisi,[4] A. Malakhov,[19] V. I. Manko,[23] Y. Mao,[37,39] G. Martinez,[45] H. Masui,[48] F. Matathias,[44] T. Matsumoto,[7,50]
M. C. McCain,[1] P. L. McGaughey,[27] Y. Miake,[48] T. E. Miller,[49] A. Milov,[44] S. Mioduszewski,[4] G. C. Mishra,[14]
J. T. Mitchell,[4] A. K. Mohanty,[3] D. P. Morrison,[4] J. M. Moss,[27] D. Mukhopadhyay,[51] M. Muniruzzaman,[5]
S. Nagamiya,[20] J. L. Nagle,[8,9] T. Nakamura,[15] J. Newby,[46] A. S. Nyanin,[23] J. Nystrand,[29] E. O'Brien,[4] C. A. Ogilvie,[18]
H. Ohnishi,[39] I. D. Ojha,[49] H. Okada,[24,39] K. Okada,[39,40] A. Oskarsson,[29] I. Otterlund,[29] K. Oyama,[7] K. Ozawa,[7] D. Pal,[51]
A. P. T. Palounek,[27] V. Pantuev,[44] V. Papavassiliou,[34] J. Park,[42] W. J. Park,[22] S. F. Pate,[34] H. Pei,[18] V. Penev,[19] J.-C. Peng,[17]
H. Pereira,[10] V. Peresedov,[19] A. Pierson,[33] C. Pinkenburg,[4] R. P. Pisani,[4] M. L. Purschke,[4] A. K. Purwar,[44] J. Qualls,[1]
J. Rak,[18] I. Ravinovich,[51] K. F. Read,[35,46] M. Reuter,[44] K. Reygers,[30] V. Riabov,[38] Y. Riabov,[38] G. Roche,[28] A. Romana,[25]
M. Rosati,[18] S. Rosendahl,[29] P. Rosnet,[28] V. L. Rykov,[39] S. S. Ryu,[52] N. Saito,[24,39,40] T. Sakaguchi,[7,50] S. Sakai,[48]
V. Samsonov,[38] L. Sanfratello,[33] R. Santo,[30] H. D. Sato,[24,39] S. Sato,[4,48] S. Sawada,[20] Y. Schutz,[45] V. Semenov,[16] R. Seto,[5]
T. K. Shea,[4] I. Shein,[16] T.-A. Shibata,[39,47] K. Shigaki,[15] M. Shimomura,[48] A. Sickles,[44] C. L. Silva,[41] D. Silvermyr,[27]
K. S. Sim,[22] A. Soldatov,[16] R. A. Soltz,[26] W. E. Sondheim,[27] S. Sorensen,[46] I. V. Sourikova,[4] F. Staley,[10] P. W. Stankus,[35]
E. Stenlund,[29] M. Stepanov,[34] A. Ster,[21] S. P. Stoll,[4] T. Sugitate,[15] J. P. Sullivan,[27] S. Takagi,[48] E. M. Takagui,[41]
A. Taketani,[39,40] K. H. Tanaka,[20] Y. Tanaka,[32] K. Tanida,[39] M. J. Tannenbaum,[4] A. Taranenko,[43] P. Tarján,[11]
T. L. Thomas,[33] M. Togawa,[24,39] J. Tojo,[39] H. Torii,[24,40] R. S. Towell,[1] V-N. Tram,[25] I. Tserruya,[51] Y. Tsuchimoto,[15]
H. Tydesjö,[29] N. Tyurin,[16] T. J. Uam,[31] H.W. van Hecke,[27] J. Velkovska,[4] M. Velkovsky,[44] V. Veszprémi,[11]
A. A. Vinogradov,[23] M. A. Volkov,[23] E. Vznuzdaev,[38] X. R. Wang,[14] Y. Watanabe,[39,40] S. N. White,[4] N. Willis,[36]
F. K. Wohn,[18] C. L. Woody,[4] W. Xie,[5] A. Yanovich,[16] S. Yokkaichi,[39,40] G. R. Young,[35] I. E. Yushmanov,[23] W. A. Zajc,[9,*]
C. Zhang,[9] S. Zhou,[6] J. Zimányi,[21] L. Zolin,[19] and X. Zong[18]

(PHENIX Collaboration)

[1]*Abilene Christian University, Abilene, Texas 79699, USA*
[2]*Institute of Physics, Academia Sinica, Taipei 11529, Taiwan*
[3]*Bhabha Atomic Research Centre, Bombay 400 085, India*

[4]Brookhaven National Laboratory, Upton, New York 11973-5000, USA
[5]University of California–Riverside, Riverside, California 92521, USA
[6]China Institute of Atomic Energy (CIAE), Beijing, People's Republic of China
[7]Center for Nuclear Study, Graduate School of Science, University of Tokyo, 7-3-1 Hongo, Bunkyo, Tokyo 113-0033, Japan
[8]University of Colorado, Boulder, Colorado 80309, USA
[9]Columbia University, New York, New York 10027, USA, and Nevis Laboratories, Irvington, New York 10533, USA
[10]Dapnia, CEA Saclay, F-91191, Gif-sur-Yvette, France
[11]Debrecen University, H-4010 Debrecen, Egyetem tér 1, Hungary
[12]ELTE, Eötvös Loránd University, H-1117 Budapest, Pázmány P. s. 1/A, Hungary
[13]Florida State University, Tallahassee, Florida 32306, USA
[14]Georgia State University, Atlanta, Georgia 30303, USA
[15]Hiroshima University, Kagamiyama, Higashi-Hiroshima 739-8526, Japan
[16]Institute for High Energy Physics (IHEP), Protvino, Russia
[17]University of Illinois at Urbana-Champaign, Urbana, Illinois 61801, USA
[18]Iowa State University, Ames, Iowa 50011, USA
[19]Joint Institute for Nuclear Research, 141980 Dubna, Moscow Region, Russia
[20]KEK, High Energy Accelerator Research Organization, Tsukuba-shi, Ibaraki-ken 305-0801, Japan
[21]KFKI Research Institute for Particle and Nuclear Physics (RMKI), H-1525 Budapest 114, P.O. Box 49, Hungary
[22]Korea University, Seoul, 136-701, Korea
[23]Russian Research Center, "Kurchatov Institute," Moscow, Russia
[24]Kyoto University, Kyoto 606, Japan
[25]Laboratoire Leprince-Ringuet, Ecole Polytechnique, CNRS-IN2P3, Route de Saclay, F-91128, Palaiseau, France
[26]Lawrence Livermore National Laboratory, Livermore, California 94550, USA
[27]Los Alamos National Laboratory, Los Alamos, New Mexico 87545, USA
[28]LPC, Université Blaise Pascal, CNRS-IN2P3, Clermont-Fd, 63177 Aubiere Cedex, France
[29]Department of Physics, Lund University, Box 118, SE-221 00 Lund, Sweden
[30]Institut fuer Kernphysik, University of Muenster, D-48149 Muenster, Germany
[31]Myongji University, Yongin, Kyonggido 449-728, Korea
[32]Nagasaki Institute of Applied Science, Nagasaki-shi, Nagasaki 851-0193, Japan
[33]University of New Mexico, Albuquerque, New Mexico, USA
[34]New Mexico State University, Las Cruces, New Mexico 88003, USA
[35]Oak Ridge National Laboratory, Oak Ridge, Tennessee 37831, USA
[36]IPN-Orsay, Universite Paris Sud, CNRS-IN2P3, BP1, F-91406, Orsay, France
[37]Peking University, Beijing, People's Republic of China
[38]PNPI, Petersburg Nuclear Physics Institute, Gatchina, Russia
[39]RIKEN (The Institute of Physical and Chemical Research), Wako, Saitama 351-0198, Japan
[40]RIKEN BNL Research Center, Brookhaven National Laboratory, Upton, New York 11973-5000, USA
[41]Universidade de São Paulo, Instituto de Física, Caixa Postal 66318, São Paulo CEP05315-970, Brazil
[42]System Electronics Laboratory, Seoul National University, Seoul, South Korea
[43]Chemistry Department, Stony Brook University, SUNY, Stony Brook, New York 11794-3400, USA
[44]Department of Physics and Astronomy, Stony Brook University, SUNY, Stony Brook, New York 11794, USA
[45]SUBATECH (Ecole des Mines de Nantes, CNRS-IN2P3, Université de Nantes) BP 20722-44307, Nantes, France
[46]University of Tennessee, Knoxville, Tennessee 37996, USA
[47]Department of Physics, Tokyo Institute of Technology, Tokyo, 152-8551, Japan
[48]Institute of Physics, University of Tsukuba, Tsukuba, Ibaraki 305, Japan
[49]Vanderbilt University, Nashville, Tennessee 37235, USA
[50]Waseda University, Advanced Research Institute for Science and Engineering, 17 Kikui-cho, Shinjuku-ku, Tokyo 162-0044, Japan
[51]Weizmann Institute, Rehovot 76100, Israel
[52]Yonsei University, IPAP, Seoul 120-749, Korea

Transverse momentum spectra of charged hadrons with $p_T < 8$ GeV/c and neutral pions with $p_T < 10$ GeV/c have been measured at midrapidity by the PHENIX experiment at BNL RHIC in $d + Au$ collisions at $\sqrt{s_{NN}} = 200$ GeV. The measured yields are compared to those in $p + p$ collisions at the same $\sqrt{s_{NN}}$ scaled up by the number of underlying nucleon-nucleon collisions in $d + Au$. The yield ratio does not show the suppression observed in central $Au + Au$ collisions at RHIC. Instead, there is a small enhancement in the yield of high momentum particles.

High transverse momentum ($p_T > 2$ GeV/c) hadrons provide an excellent probe of the high energy density matter created in relativistic heavy ion collisions [1,2]. They arise from fragmentation of quarks and gluons (partons) scattered with large momentum transfer, Q^2, in the initial parton-parton interactions [3]. In the

absence of medium effects, these hard scattering yields in nucleus-nucleus collisions should scale with the average number of inelastic nucleon-nucleon collisions N_{coll} (binary scaling). One of the most intriguing observations from experiments at the BNL Relativistic Heavy Ion Collider (RHIC) is the large suppression of high p_T neutral pion and charged hadron yields in central Au + Au collisions with respect to $p + p$ results scaled by the number of binary nucleon-nucleon collisions [4–7].

Theoretical studies of parton propagation in high density matter suggest that partons lose a significant fraction of their energy through gluon bremsstrahlung [1,2], reducing the parton momentum and depleting the yield of high p_T hadrons [8–13]. This is a final-state effect in the spatially extended medium created in $A + A$ collisions. Initial-state effects include nuclear modifications to the parton momentum distributions (structure functions), and soft scatterings of the incoming parton prior to its hard scattering. These should be present in $p + A$, $d + A$, and $A + A$. Interpretations of Au + Au collisions based on initial-state parton saturation effects [14] or final-state hadronic interactions [15] also predict a considerable suppression of the hadron production at high p_T. It is therefore of paramount interest to determine experimentally the modification, if any, of high p_T hadron yields due to initial-state nuclear effects for a system in which a hot, dense medium is not produced in the final state. This Letter reports on charged hadron and π^0 production at midrapidity obtained by the PHENIX [16] experiment at RHIC in $d + Au$ collisions at $\sqrt{s_{NN}} = 200$ GeV. The results are compared to those in $p + p$ and Au + Au [7,17,18] at the same nucleon-nucleon center-of-mass energy. Similar $d + Au$ measurements are also reported in [19,20].

The data were collected under two different trigger conditions. Minimum bias events with vertex position along the beam axis within $|z| < 30$ cm were triggered by the beam-beam counters (BBC) [16] which cover $|\eta| = 3.0$–3.9. The minimum bias trigger accepts $(88\% \pm 4\%)$ of all inelastic $d + Au$ collisions that satisfy the vertex condition. A total of 1.2×10^7 and 1.7×10^7 events were analyzed for charged hadron and π^0 spectra, respectively. A second "photon triggered" sample, requiring showers above 2.5 GeV for lead-scintillator (PbSc) and 3.5 GeV for lead-glass (PbGl) electromagnetic calorimeters (EMCal) [16] in addition to the BBC requirement, is used to extend the π^0 measurements to higher p_T. This trigger sampled a total of 1.7×10^9 events.

Neutral pions were measured by the PHENIX EMCal via the $\pi^0 \rightarrow \gamma\gamma$ decay. The EMCal covers $|\eta| \leq 0.35$ in pseudorapidity and $\Delta\phi = \pi$ in azimuth. It consists of six PbSc and two PbGl sectors, each covering $\pi/8$ in azimuth. The data from PbSc and PbGl were analyzed separately. The energy calibration is obtained from beam tests, cosmic rays, minimum ionizing energy peaks of charged hadrons, and the energy/momentum ratio of

electrons identified with the Ring Imaging Čerenkov Detector. The combined uncertainty on the energy scale and linearity is $\leq 1.5\%$, determined from the response to identified electrons, and confirmed by the positions and widths of the observed π^0 mass peaks.

Photonlike energy clusters in the calorimeter are selected via shower profile cuts. The invariant mass for all photon pairs with energy asymmetry $|E_1 - E_2|/(E_1 + E_2) < 0.7$ is calculated and binned in p_T. The π^0 yield in each p_T bin is determined by integrating the background subtracted two-photon invariant mass distribution [7]; the background is determined from mixed events. The peak-to-background ratio increases from ~0.3 at $p_T = 1.25$ GeV/c to more than 5 above 4.25 GeV/c. The raw π^0 spectra are corrected by Monte Carlo simulations for trigger efficiency and acceptance, and for π^0 reconstruction efficiency including dead areas, effects of energy resolution, photon identification cuts, and peak extraction window. Finally, the yields are corrected to the center of the p_T bin using the observed slope of the spectrum. Below $p_T = 5$ GeV/c the yields are determined from the minimum bias data sample while above 5 GeV/c the photon triggered sample is used. The main sources of systematic errors are listed in Table I. The final systematic errors on the spectra are 10% to 16%, increasing with p_T.

Charged particles are reconstructed using a drift chamber (DC) followed by two layers of multiwire proportional chambers with pad readout (PC1, PC3) [16]. In this analysis tracks were reconstructed over a restricted pseudorapidity range $|\eta| < 0.18$. Pattern recognition in the DC is based on a combinatorial Hough transform in the track bend plane, while the polar angle is determined by PC1 and the location of the collision vertex along the beam direction [21]. The vertex was constrained to be within $|z| < 18$ cm for analysis of the charged tracks. The track reconstruction efficiency is approximately 98%, independent of p_T. Particle momenta are measured with

TABLE I. Systematic errors in percent on π^0 invariant yields for PbSc (PbGl), as a function of p_T (in GeV/c). There are three categories of uncertainty: Type A is a point-to-point error uncorrelated between p_T bins, type B is p_T correlated, where all points move in the same direction but not by the same factor, while in type C all points move by the same factor independent of p_T.

	Type	$p_T = 2$	$p_T = 6$	$p_T = 10$
Peak extraction	A	5.0(5.0)	5.0(5.0)	5.0(5.0)
Geom. accept.	B	3.0(3.0)	2.0(2.0)	2.0(2.0)
π^0 reconstr. eff.	B	4.0(4.0)	4.0(4.0)	4.5(4.5)
Energy scale	B	4.0(4.0)	9.0(9.0)	11.0(11.0)
Trigger eff.	B	$\cdots$	5.0(10.0)	3.0(3.0)
Trigger norm.	C	$\cdots$	5.0(5.0)	5.0(5.0)
Conversion corr.	C	2.8(2.8)	2.8(2.8)	2.8(2.8)
Total error		8.6(8.6)	14(16)	15(15)

a resolution $\delta p/p = 0.7\% \oplus 1.1\% p$ (GeV/c). The momentum scale is known to 0.7%, from the reconstructed proton mass using the time of flight. A confirmation hit is required in PC3, located at a radius of 5 m, within a 2.5σ matching window to eliminate most albedo, conversions, and decays. The remaining background above $p_T = 5$ GeV/c is subtracted statistically using identified conversions and weak decays (primarily kaons) [18].

Corrections to the charged particle spectrum for geometrical acceptance, decays in flight, reconstruction efficiency, and momentum resolution are determined using a single-particle GEANT Monte Carlo simulation. All analysis steps, including the outer detector matching cuts are applied consistently in simulation and data. As the DC and PC occupancies in $d + \mathrm{Au}$ are low, no multiplicity-dependent occupancy corrections are required. The yield was corrected to the center of the p_T bin. Table II lists the source and magnitude of each contribution to the systematic uncertainties on the charged particle spectra.

The fully corrected p_T distributions of π^0's and $(h^+ + h^-)/2$ are shown in Fig. 1. Each panel shows the reference spectrum from $p + p$ collisions along with the particle spectrum from $d + \mathrm{Au}$. The reference for π^0 is the π^0 spectrum measured in $p + p$ by PHENIX [17], shown on the right panel. For charged hadrons, the reference is obtained by scaling up the π^0 spectrum by the p_T-dependent h/π ratio observed at the CERN Intersecting Storage Rings [22] at $\sqrt{s} = 23$ to 63 GeV and measured by PHENIX. The value of h/π is constant at 1.6 ± 0.16 above 1.5 GeV/c, and decreases at lower p_T to a value of $1.25^{+0.12}_{-0.25}$. Table III summarizes uncertainties on the reference spectra.

A standard way to quantify nuclear medium effects on high p_T production is by the *nuclear modification factor,* which we define for $d + \mathrm{Au}$ collisions as the ratio of invariant yield in $d + \mathrm{Au}$ to that of $p + p$, scaled by the number of binary collisions.

$$R_{dA}(p_T) = \frac{(1/N_{dA}^{\mathrm{evt}})\,d^2 N_{dA}/d\eta\,dp_T}{\langle N_{\mathrm{coll}}\rangle/\sigma_{pp}^{\mathrm{inel}}\,d^2\sigma_{pp}/d\eta\,dp_T},$$

where $\langle N_{\mathrm{coll}}\rangle$ is the average number of inelastic nucleon-nucleon (NN) collisions per event in the minimum bias
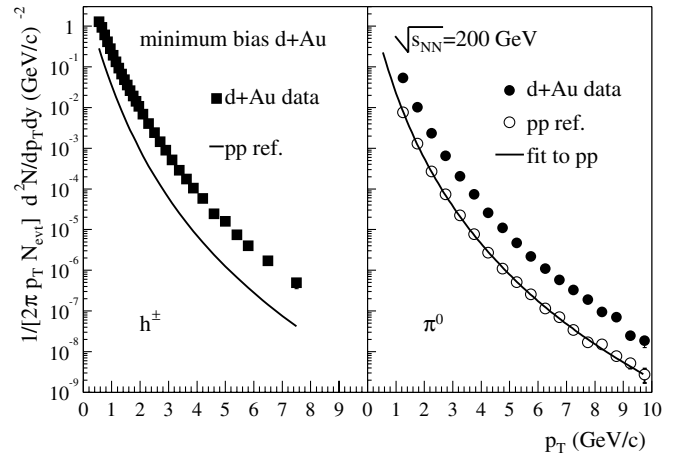

FIG. 1. Midrapidity p_T spectra for charged hadrons and π^0. Total uncertainties are shown. The π^0 below 5 GeV/c are from minimum bias triggered events, and above from photon triggered events. Lines show fits to reference spectra from $p + p$ collisions, and open points show the $p + p$ π^0 spectrum measured by PHENIX [17].

collisions, and $\langle N_{\mathrm{coll}}\rangle/\sigma_{pp}^{\mathrm{inel}}$ is the nuclear overlap function $\langle T_{dA}(b)\rangle$. Using a Glauber model [23] and simulation of the BBC, $\langle N_{\mathrm{coll}}\rangle$ is 8.5 ± 0.4 in minimum bias $d + \mathrm{Au}$.

The ratio R_{dA} is plotted separately for π^0 measured in the PbGl and in the PbSc calorimeters in Fig. 2. The two analyses are consistent within errors. The data are compared to the corresponding nuclear modification factor R_{AA} obtained from central $\mathrm{Au} + \mathrm{Au}$ collisions. The top panel of Fig. 3 shows R_{dA} for inclusive charged particles $(h^+ + h^-)/2$, again compared with R_{AA} observed in central $\mathrm{Au} + \mathrm{Au}$ collisions, while the lower panel compares $(h^+ + h^-)/2$ with π^0. In both Figs. 2 and 3, the uncertainties are plotted as follows: error bars represent the quadrature sum of statistical errors and those systematic errors which vary point to point in p_T; systematic errors on the absolute yield and the systematic errors which are correlated point to point are shown as bands. All procedures for estimating the various systematic errors have been adjusted to provide estimates corresponding to 1σ error values.

The data clearly indicate that there is no suppression of high p_T particles in $d + \mathrm{Au}$ collisions. We do, however, observe an enhancement in inclusive charged particle production at $p_T > 2$ GeV/c. A similar enhancement

TABLE II. Systematic errors in percent on the $(h^+ + h^-)/2$ invariant yields. Error types are as in Table I.

	Type	$p_T < 4$	$p_T = 4$	$p_T = 6$	$p_T = 7$
PC3 match	C	2.4	2.4	2.4	2.4
Geometr. acc.	C	2.9	2.9	2.9	2.9
Monte Carlo corr.	C	3.7	3.7	3.7	3.7
Mom. resolution	B	$\cdots$	<0.5	0.6	1.2
Mom. scale	B	<3.2	3.2	3.5	3.7
Backgd. subtrac.	B	<0.5	0.6	3.8	8.2
π oversubtrac.	B	$\cdots$	$\cdots$	1.8	4.7
Total error		6.2	6.2	7.6	11.5

TABLE III. Systematic errors on the $p + p$ reference spectrum.

	Type	$p_T < 2$	$p_T = 4$	$p_T = 6$	$p_T = 10$
Normalization	C	10	10	10	10
Residual syst.	B	3	5	7	9
Charged (π^0) only[a]	B(A)	8(5)	7(5)	9(5)	20(5)

[a]Errors affect only the charged (neutral) analysis, and include h/π_0, and fits to reference (point by point pp) errors.
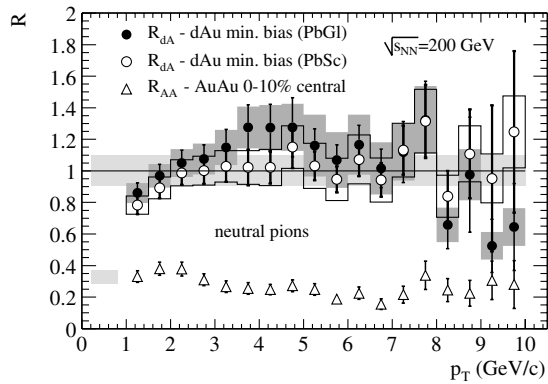
FIG. 2. Nuclear modification factor R_{dA} for π^0 in the PbGl and PbSc calorimeters in minimum bias $d + $ Au. The bands around the data points show systematic errors which can vary with p_T, while the shaded band around unity indicates the normalization uncertainty. The nuclear modification factor R_{AA} in 10% most central Au $+$ Au collisions is also shown.

was observed in $p + A$ fixed-target experiments [24] and is generally referred to as the "Cronin effect." To facilitate comparison of the Cronin effect in inclusive charged particles and π^0, the lower part of Fig. 3 shows all systematic uncertainties common to both analyses in the
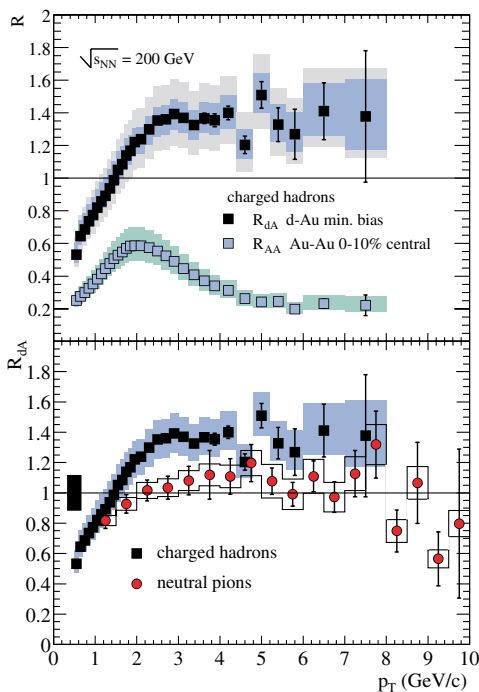

FIG. 3 (color online). Top: Nuclear modification factor R_{dA} for $(h^+ + h^-)/2$ in minimum bias $d + $ Au compared to R_{AA} in the 10% most central Au $+$ Au collisions. Inner bands show systematic errors which can vary with p_T, and outer bands include also the normalization uncertainty. Bottom: Comparison of R_{dA} for $(h^+ + h^-)/2$ and the average of the π^0 measurements in $d + $ Au. The bar at the left indicates the systematic uncertainty in common for the charged and π^0 measurements.

bar on the left. It should be noted that this uncertainty must be added in quadrature with the bands shown for each curve to obtain the 1σ allowed range of R_{dA} from the data. The π^0 data suggest a smaller enhancement for pions than for inclusive charged particles at $p_T = $ 2–4 GeV/c. We note that the charged spectrum includes baryons and antibaryons, which may have a different nuclear enhancement than the mesons [24].

The various models of the suppression observed in Au $+$ Au predict a different dependence on N_{coll} in $d + $ Au [14,25,26]. Therefore, a second data sample was selected by requiring observation of a neutron in the zero-degree calorimeter on the deuteron-going side of PHENIX. This, together with the requirement of particles entering both beam-beam counters, selects a class of events in which only the proton from the deuteron interacts with the Au nucleus. The mean number of binary collisions for this sample is calculated with the Glauber model to be 3.6 ± 0.3. Particle yields in this sample have a $<5\%$ uncertainty beyond that of the minimum bias sample, arising from trigger bias.

Figure 4 shows the ratios of R_{dA} in minimum bias $d + $ Au to R_{pA} in the neutron tagged sample, for both $(h^+ + h^-)/2$ and π^0. Systematic uncertainties on the spectra cancel in the ratio; the band around unity shows the uncertainty on the ratio of the number of binary collisions in the two samples. Average values of N_{coll} are 3.6 per participating proton in the neutron tagged sample and 8.5 for 1.7 participating nucleons from the deuteron in minimum bias $d + $ Au. Given the systematic uncertainties on N_{coll}, we cannot exclude a small centrality dependence for $p_T > 1$ GeV/c. It should be noted that the figure also indicates that $d + $ Au collisions provide a good measure of the physics of $p + $ Au.

The observation of an enhancement of high-p_T hadron production in both the minimum bias $d + $ Au and the neutron tagged sample of $p + $ Au collisions indicates that the suppression in central Au $+$ Au collisions is not an initial-state effect. Nor does it arise from modification of parton structure functions in nuclei. The data suggest,
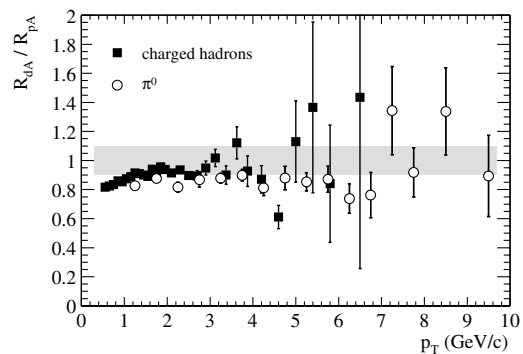

FIG. 4. Ratio of R_{dA} in minimum bias $d + $ Au and R_{pA} from neutron tagged $d + $ Au collisions for $(h^+ + h^-)/2$ and π^0. The band shows the uncertainty on the number of binary collisions; all other systematic errors cancel.

instead, that the suppression of high p_T hadrons in Au + Au is more likely a final-state effect of the produced dense medium.

*PHENIX spokesperson.
Email address: zajc@nevis.columbia.edu

[1] M. Gyulassy and M. Plümer, Phys. Lett. B **243**, 432 (1990); X. N. Wang and M. Gyulassy, Phys. Rev. Lett. **68**, 1480 (1992).
[2] R. Baier et al., Phys. Lett. B **345**, 277 (1995).
[3] J. F. Owens et al., Phys. Rev. D **18**, 1501 (1978).
[4] K. Adcox et al., Phys. Rev. Lett. **88**, 022301 (2002).
[5] K. Adcox et al., Phys. Lett. B **561**, 82 (2003).
[6] C. Adler et al., Phys. Rev. Lett. **89**, 202301 (2002).
[7] S. S. Adler et al., nucl-ex/0304022 (to be published).
[8] M. Gyulassy and X. N. Wang, Nucl. Phys. **B420**, 583 (1994); X. N. Wang, Phys. Rev. C **58**, 2321 (1998).
[9] I. Vitev and M. Gyulassy, Phys. Rev. Lett. **89**, 252301 (2002).
[10] S. Jeon, J. Jalilian-Marian, and I. Sarcevic, Phys. Lett. B **562**, 45 (2003).
[11] G. G. Barnaföldi et al., nucl-th/0212111; V. Greco, C. M. Ko, and P. Lévai, Phys. Rev. Lett. **90**, 202302 (2003).
[12] X. N. Wang, Nucl. Phys. **A715**, 775 (2003).
[13] F. Arleo, J. High Energy Phys. 11 (2002) 044.
[14] D. Kharzeev, E. Levin, and L. McLerran, Phys. Lett. B **561**, 93 (2003).
[15] K. Gallmeister, C. Greiner, and Z. Xu, Phys. Rev. C **67**, 044905 (2003).
[16] K. Adcox et al., Nucl. Instrum. Methods Phys. Res., Sect. A **499**, 469 (2003), and references therein.
[17] S. S. Adler et al., hep-ex/0304038 (to be published).
[18] J. Jia et al., Nucl. Phys. **A715**, 769c (2003).
[19] J. Adams et al., Phys. Rev. Lett. **91**, 072304 (2003).
[20] B. B. Back et al., Phys. Rev. Lett. **91**, 072302 (2003).
[21] J. T. Mitchell et al., Nucl. Instrum. Methods Phys. Res., Sect. A **482**, 491 (2002).
[22] B. Alper et al., Nucl. Phys. **B100**, 237 (1975).
[23] In the present work the Woods-Saxon nuclear density parameters radius $R = 6.38$ fm, diffusivity $a = 0.54$ fm, and N-N cross section $\sigma_{NN}^{\rm inel} = 42$ mb were used. The deuteron is described by a Hulthén wave function [L. Hulthén and M. Sugawara, Handb. Phys. **39** 1 (1957)] with $\alpha = 0.228$ fm^{-1} and $\beta = 1.18$ fm^{-1}.
[24] D. Antreasyan et al., Phys. Rev. D **19**, 764 (1979).
[25] I. Vitev, Phys. Lett. B **562**, 36 (2003).
[26] B. Kopeliovich, Phys. Rev. Lett. **88**, 232303 (2002).